Neurophysiology, Vol. 41, No. 1, 2009

Functional Mixed-Effect Models for Electrophysiological Responses

D. J. Davidson[1]

Neirofiziologiya/Neurophysiology, Vol. 41, No. 1, pp. 79-87, January-February, 2009.

Received October 2, 2008.

In electro/psychophysiological experiments, linear mixed-effect modeling is an effective statistical technique for data repeatedly observed from the same experimental participants or stimulus items. This review describes the application of mixed-effect modeling to functional responses, in particular those observed in event-related EEG or MEG experiments, using a discrete wavelet transform. The technique is illustrated with a design with several covariates, and procedures for generating posterior samples and computing a Bayesian false discovery rate are described.

Keywords: evoked potentials, mixed-effect analysis, wavelet, false discovery rate, stochastic process.

INTRODUCTION

Event-related potentials (ERPs) recorded using electroencephalography (EEG) or magnetoencephalography (MEG) are routinely used in the studies of cortical activity related to cognitive tasks [1-3] and are also applied to the analysis of local field potentials and electrocorticograms. The time resolution of the ERP technique allows certain aspects of cortical activity to be studied with relatively high temporal resolution. This can be used, e.g., for examination of electrophysiological reactions induced by presentation of a single word embedded within a sentence, as well as many other types of time-limited cerebral activity. However, a persistent problem with this approach is that the magnitude of the ERP is usually very small compared to the noise or the unmodeled activity; the latter is inevitably present in individual trials. This activity often substantially varies from one experimental participant to another, complicating estimation and inference for "useful" responses. Outside of electrophysiology, statistical techniques, such as mixed-effect linear modeling, have been used for improved statistical treatment of the participant heterogeneity [4, 5], but the mixed-effect approach is not yet commonly applied to time series analysis in EEG experiments. This paper describes the application of a wavelet-based functional mixed-effect model (WFMM) developed by Morris and Carroll [6] to EEG data for the purpose of regression analysis of ERPs. This technique provides a flexible model of fixed and random effects, as well as a method to limit the false discovery rate (FDR) for statistical contrasts of time series.

A wavelet is a limited-duration function with an oscillatory pattern, which can be used to provide local analysis of the signal energy in nonstationary signals ([7-9], for introduction see [8, 9]). For a signal X_k = = ($x1x2$ ... xk), let $k = 2^J$, where J is a positive integer denoting the scale of the analysis. The discrete wavelet transform (DWT) can be described as the recursive application of high-pass (h_l) and low-pass (g_l) filters to X_k (1 and 2) followed by downsampling. The filter coefficients depend on the family of wavelets that are employed.

$$a_{J-1,k} = \Sigma_m h_{m-2k} a_{J,m} \quad (1)$$

$$d_{J-1,k} = \Sigma_m g_{m-2k} a_{J,m} . \quad (2)$$

The coefficients $a_{J-1,k}$ are termed *scaling* coefficients at the scale J–1 and time index k, and the $d_{J-1,k}$ are termed *detail* coefficients at the scale J–1 and time index k.

[1] Max Planck Institute for Human Cognitive and Brain Sciences, Leipzig, Germany.
Correspondence should be addressed to D. J. Davidson (e-mail: davidson@cbs.mpg.de).

The low-pass filter coefficients g_l can be defined as $g_l = = (-1)^1 h_{l-1}$. The DWT can be represented in the form of a matrix computation, D = WY, where W is an orthogonal matrix with the wavelet filter coefficients. Applying W to a time series in the data matrix Y, a matrix D of detail and approximation coefficients is obtained. This matrix D can be used to parameterize a model of the stochastic process investigated in an EEG experiment. It captures nonstationary response properties via the location of the wavelet coefficients, which capture the translation of the analysis wavelet function in time. It also captures the scale, which refers to the extent of the analysis function over time. The arrangement of these two parameters allows a wavelet analysis to jointly capture both global and local signal patterns with some degree of temporal localization. This approach is well-suited to modeling the chirp-like character often seen in the observed ERP responses, which often contain early shorter timescale components followed by longer timescale components at later time intervals (see Fig. 1A for an example).

Wavelets are now widely applied to EEG analyses to characterize time-varying properties of the unaveraged EEG signal [10, 11], as well as to address the issue of noise in ERP estimations [12]. With regard to the analysis of the ERP itself, Bertrand et al. [13] were one of the first who proposed to analyze ERP responses with the DWT and described the relation between the estimates and the continuous wavelet transform (see also [14, 15]). Demiralp et al. [16] used a wavelet based on quadratic B-splines to analyze late cognitive components in ERPs. Their approach treated each coefficient (at each scale and time) as a separate random variable, which they analyzed using repeated ANOVA measures. This analysis takes into account the subject variability in the wavelet coefficients when characterizing the population estimates of the wavelet coefficients. This subject variability in either the ERP response or the background activity may have a substantial impact on the sensitivity of wavelet analysis for later components, which would be expected to be more variable than the earlier sensory-related components. More recently, Kiebel and Friston [17] proposed a hierarchical observation model of ERP responses based on analyses of either fixed or random effects. Also, Raz et al. [18] proposed a random-effect inferential scheme for ERP analysis based on wavelets, which is conceptually similar to the model adopted here (see also recent work by Wang and colleagues [19]).

From a statistical perspective, the wavelet transform is popular for denoising because of a decorrelating property of the wavelet coefficients [20]. The assumption is that the energy of the signal will be concentrated in a small number of wavelet coefficients, while Gaussian noise is evenly dispersed over the remaining coefficients. If these assumptions hold, then an EEG signal might be denoised by reducing the magnitude of small coefficients. Using a DWT, the procedure consists of transforming the EEG signal into the wavelet domain, shrinking relatively small coefficients towards zero and then using an inverse discrete wavelet transform (IDWT) to project the signal back to the data domain; this allows one to obtain a denoised signal. The scope of the present paper will be limited to the use of wavelets to denoise the ERPs and leaves for future work the application of mixed-effect analysis to the time/frequency power distribution of the unaverged EEG signals.

There have been several recent approaches to EEG or MEG signal analysis, which have exploited wavelets for this type of noise reduction. Quian Quiroga and Garcia [21] showed that thresholding the wavelet coefficients to zero and subsequently using an inverse DWT allow one to obtain improved averaged ERP estimates. They also suggested that once wavelet coefficients for this denoising analysis are chosen, the method does not require heuristic assessment. Wang et al. [22] also demonstrated that wavelet denoising can improve ERP estimates when *a priori* knowledge of the components is available. Related work by Effern et al. [23] compared wavelet, combined Woody-filtering and wavelets, and *a posteriori* Wiener filtering for the analysis of single-trial data (see also [24, 25]). As in the previous work, they showed that signal estimation was improved when wavelet denoising has been applied, and that the wavelet approaches have certain advantages over other approaches. However, they did not place the estimation procedure in a statistical framework to account for subject variability. When embedded in an inferential framework, the choice of wavelet coefficients for shrinkage could also be seen as elicitation of priors in an empirical Bayesian analysis. In general, the use of these techniques has considerable theoretical relevance, as there is persistent debate regarding how the functional EEG response should be modeled [26, 27].

The linear regression of multiple covariates has been applied to ERP responses by Hauk et al. [28, 29], but not using denoising wavelet analysis or mixed-effect modeling. Other related works included several applications of wavelets to functional neuroimaging data [30] (Fadili and Bullmore [31] provided an overview). For example, Sendur et al. [32] introduced

a resampling method based on a DWT to improve statistical testing of statistical parametric maps.

Finally, there is an issue of false discovery rates. ERP difference waveforms are sometimes calculated in order to find the onset and/or offset of a response when comparing an active period to a baseline, or a difference between the responses obtained under two different conditions. This difference can be evaluated using a point-by-point confidence interval for the difference, based on the standard error of the difference between the waveforms (e.g., [33]). However, there is a multiple-comparison problem if there is a large number of time points to compare [34-36]. Corrections for multiple comparisons reduce the sensitivity of the test in order to control the false alarm rate, and this problem is multiplied if samples recorded either by many electrodes or under many conditions should be compared. One approach to this problem is to adopt non-parametric permutation tests [37]. Another approach (described in the present paper) is to calculate a Bayesian FDR for providing the difference contrast computed with the functional mixed-effect model.

The aim of this review is to illustrate the application of the WFMM developed by Morris and Carroll [6] to the electrophysiological data. While conceptually similar approaches have been advanced from a variety of theoretical perspectives, the novel aspects of the approach outlined here are that (*i*) it embeds the wavelet denoising procedure in an explicit inferential framework, and (*ii*) it allows the computation of a Bayesian FDR for a response time series associated with a regressor in the design matrix for an experiment. This can be used to model single fixed effects or interactions in functional terms. The application is illustrated with an experimental design that includes random effects for subjects and covariates for properties of the stimulus items. In the following, a brief description of the mixed-effect approach is provided, along with the extension of this to functional data analysis. Finally, the example analysis is used to illustrate the technique, and this is followed by several discussion points.

METHODS

Fixed and Random Effects. The linear mixed-effect model approach simulates a response as a function of fixed and random effects, as well as a noise term, as in Eq. (3) below (the notation similar to Laird and Ware [38]). This approach treats each observation as a single point; it can be applied to ERP analysis to model the mean amplitude of the response within a pre-defined time interval, e.g.,

$$y = X\beta + Zb + \varepsilon,\ \varepsilon \sim N(0,\sigma^2 I),\ b \sim N(0,\Psi),\ \varepsilon \perp b, \quad (3)$$

where y are N samples of the response variable, X is the $N \times p$ design matrix for the fixed effects, β is the $p \times 1$ column vector of fixed-effect coefficients, Z is the $N \times m$ design matrix for the random effects, b is the $m \times 1$ matrix of the random-effect coefficients, and ε is the $N \times 1$ column vector of the residual error. The random-effect coefficients b and residual error ε are distributed according to Ψ, the variance-covariance matrix of the random effects.

In the case where the design matrix Z models a single grouping factor, such as experimental participants, the model is qualified as having a single random effect. When there is more than one grouping factor, Z is subdivided into blocks, which capture the correlations between and within the grouping factors.

If a participant is presented with a set of stimuli, then the responses to those stimuli are likely to be more similar to each other than to the responses of a different participant. This correlation is captured with the grouping factor. Likewise, if a stimulus word is presented to a set of participants, the responses to that word may be more similar to each other than to a different word. Thus, either participants or items can be grouping factors. When each participant is presented with each stimulus item, then these two random effects are said to be fully crossed. Depending on the distribution of items to participants within the design, other relationships are possible, such as nesting of items within separate groups of participants.

Functional Mixed-Effect Models. The functional mixed-effect model generalizes the linear mixed-effect approach to functional analysis. This treats the response vector as a time series ([6, 39, 40]; for an application to physiological data see [41, 42]). To model electrophysiological data, the mixed-effect model in Eq. (3) is replaced by a form that includes the time parameter in Eq. (4).

$$y(t) = X\beta(t) + Zb(t) + \varepsilon(t),\ \varepsilon \sim MN(P,Q),\ b \sim MN(R,S), \quad (4)$$

where $y(t) = y_1(t), y_2(t) \ldots y_n(t)$ are samples of N observed time series, arranged so that each observed time series is a row. Each time series is observed for $t = t_1, \ldots, t_n$ time points of the length T, and, therefore, the matrix Y is $N \times T$, X is the $N \times p$ design matrix for the

fixed effects, β(t) is the $p \times T$ matrix of fixed-effect coefficients in the functional form, Z is the $N \times m$ design matrix for the random-effects, b(t) is the $m \times T$ matrix of random-effect coefficients in the functional form, and ε(t) is the $N \times T$ matrix of a residual error process. The random-effect functions b(t) and residual error process ε(t) are assumed to be distributed according to the Matrix Normal (MN) distribution [43], P and R are the $m \times m$ covariance matrices, and Q and S are the (diagonal) $T \times T$ covariance matrices.

Within the framework of the WFMM approach, β(t) and b(t) are modeled with the wavelet coefficients obtained by applying a DWT to the time series of each trial with a discrete matrix version of Eq. (4), as in Eq. (5)

$$Y = XB + ZU + E, \quad (5)$$

where Y, X, B, Z, and E are the matrices of the same order as in Eq. (4). The matrix U is of order $m \times T$, where each row contains a random-effect function on the same time interval as the fixed-effect functions, corresponding to b(t) in Eq. (4). The rows of U and E are assumed to be independently and identically distributed matrix variate normal distributions, $MVN(0,Q)$ and $MVN(0,S)$, respectively. Both Q and S are the $T \times T$ discrete-form covariance matrices. The wavelet coefficients are obtained by applying a DWT projection matrix W′ to each row of Y to provide a row vector of the wavelet coefficients d,

$$d = yW'. \quad (6)$$

The estimation is done using Markov Chain Monte Carlo (MCMC) re-sampling, which is used to get posterior samples of the functions β and b, as well as the covariance matrices. In broad terms, the MCMC procedure proceeds via three steps: (1) Gibbs sampling of the fixed-effect function coefficients conditioned by the variance components and the data, (2) Metropolis-Hasting sampling of the variance components conditioned on the fixed-effect functions and the data, and when there are random effects in the model, and (3) Gibbs sampling from the random-effect distribution given the fixed effect functions, their variances, and the data. Finally, the wavelet coefficients are projected back to the data domain with an IDWT via W, which is the transpose of the original projection matrix. The result of the model is a posterior sample of the fixed-effect functions, fixed-effect variances, and pointwise posterior credible intervals. Applied to the EEG data, the design matrices X and Z capture the variables in the experimental task and any covariates introduced to the functional response. The fixed effects estimated from the model include a set of the curves for each of the fixed-effect regressors in the model, their variances, and intervals. MCMC samples of the covariance matrices Q and S are obtained from a 2D IDWT applied to the covariance matrices in the wavelet space.

The WFMM analysis allows one to shrink small wavelet coefficients in a Bayesian framework. Shrinkage (independent mixture) priors are placed on $\beta(t)$, and vague priors are placed on the covariance matrices P, Q, R, and S. Morris and Carroll [6] used a scheme in which the prior for the wavelet coefficients at the scale j and time k for the fixed effect function i, $B_{ijk} = \gamma_{ijk} Normal(0,\tau_{ij}) + (1 - \gamma_{ijk})\delta_0$, where γ_{ijk} $Bernoulli(\pi_{ij})$ and where δ_0 is a delta function located at zero. This use of a (mixture) prior results in shrinkage of the posterior estimates of the wavelet coefficients B_{ijk}. There are two regularization parameters associated with this prior, τ_{ij} and π_{ij}, which, in the Morris and Caroll approach [6], were specified mechanistically with an empirical Bayes procedure.

A Bayesian FDR is calculated by summing the posterior samples from the MCMC simulation ([44], section 4), assuming an effect size of at least the magnitude δ. For the posterior samples of the fixed-effect functions B, the point-for-point posterior probabilities of an effect exceeding δ are computed. This is done by replacing each point of the posterior samples exceeding δ by a constant that depends on the number of samples of the fixed-effect functions calculated, and by replacing the rest of the set by zero. Then, for some choice of the FDR, the time points are sorted in a descending order, and a threshold is identified to find the maximum value of the response within the FDR.

APPLICATION EXAMPLES

Data. The data for the application example consist of EEG trials collected in a previously reported sentence-processing experiment carried out in Dutch (see [45] for further details). In that experiment, subjects read sentences presented at the center of a CRT monitor in the mode of one word at a time. The data analyzed here are from two of the conditions of the experiment, comparing trials with a semantic violation *vs* a control. The contrast between the semantic violation (a critical word, CW) relative to the control was expected to yield an effect on the N400 wave form [46] within a

time interval of approximately 0.3 to 0.5 sec, and this was confirmed earlier [45]. The task for the subjects (n = 20) was to indicate whether the sentence was sensible or not after the sentence had been completed. The EEG response was measured from presentation of a CW within the sentence, which in the violation sentences was the first word that rendered the sentence nonsensical (e.g., *trees* in *The students could speak many trees*), and in the control sentences was the corresponding word in a sensible context (e.g., *trees* in *The wind swept through the trees*). The stimulus items consisted of a list of 90 well-formed Dutch sentences, each containing one noun designated as a CW, as in the example. The set of 90 violation sentences was created by exchanging the CWs of the well-formed sentence to create a nonsensical version. Each participant saw 45 of the sentences in the control version and other 45 sentences from the violation version, so that no participant saw the same sentence in both versions.

The response time series was taken from the EEG data within an interval of –0.2 to 0.8 sec from the onset of the CW; these data were averaged over five channels that were expected to include the N400 response (these included a Cz lead and four other adjacent electrodes approximately 1 cm from Cz). A low-pass 4th-order Butterworth filter at 30 Hz was applied prior to the data analysis, and for each trial the mean of a baseline interval from –0.1 to 0.0 sec was subtracted from the entire time series for the trial. Artifact trials were identified and rejected using a threshold set at ±150 μV. The data were sampled during recording at 1 kHz and downsampled to 256 Hz for the analysis, so the resulting time series was T = 256 time points. Some trials were lost because of artifact rejection, leaving 1652 trials in total, and 41.2 ± ± 2.2 (M ± s.d.) violation trials and 41.4 ± 2.4 control trials per participant, on average. To reiterate, the purpose of the present analysis is to illustrate how the functional mixed-effect regression might be applied to an already well-known response contrast, as well as to illustrate how additional regressors can be added.

RESULTS

The data matrix Y was modeled with the functional model in Eq. (5). The fixed-effect design matrix X included an intercept term for the grand mean ERP response, and the contrast between violation and control conditions, as well as three additional main effect covariates: (i) trial block (13) corresponding to three blocks of 30 trials, (ii) critical word length ranged from 4 to 15 characters, and (iii) word frequency estimated using the log-word form of the frequency from the Celex database [47]. Each of the additional variables was standardized by subtracting the mean and dividing by one standard deviation. Thus, X had dimensions 1652 × 5. The random-effect design matrix Z consisted of a dummy-coding matrix identifying the subject (corresponding to the trials in Y) and had the dimension 1652×20.

The WFMM analysis used a Daubechies discrete wavelet basis (known as *db4* in Matlab notion) with J = 8 levels of decomposition, a periodic boundary correction in an extended mode, and no compression. Using MCMC, 5000 samples of the fixed-effect functions were obtained, with a burn-in of 1000 samples. The level a for the FDR was set at 10%, and the minimum effect size d was set at 0.1 μV.

Figure 1A shows the grand averaged ERP response based on the WFMM analysis. Figure 1B shows that the variance function follows the main amplitude fluctuation of the grand averaged ERP, with most of the variance concentrated from 0.1 to 0.4 sec with a low variance from 0.4 to approximately 0.6 sec. The within-subject correlation matrix in Fig. 1C shows that the time points around the time of the stimulus-related N100-P200 complex were in weak positive correlation with other time points. This suggests that the stimulus-related amplitude fluctuation is not strongly related to the changes at later times. Also, the time points from approximately 0.2 until 0.4 sec more strongly positively correlated with each other as a block but somewhat negatively correlated with the block from 0.5 sec until the end of the response interval. This is consistent with the main pattern of the grand averaged ERP, which appears as a slow oscillatory pattern from 0.2 until 0.8 sec. The oscillatory pattern of the ERP appears to be reflected in the alternating blocks of positive/negative correlations in the correlation matrix. The residual error surface in Fig. 1D shows broadly positive correlations decreasing as a function of time.

The main contribution of the WFMM approach is its ability to flexibly model several fixed-effect regressors for a response observed in an experiment, including credibility intervals for the functional form of each effect. Figure 2 shows the response contrasts for the covariates included in the WFMM analysis. A 95% significance interval is plotted above and below the fixed-effect functions, and time points exceeding the FDR are indicated with solid dots. Figure 2A shows the negative potential difference between responses with respect to the control and violation

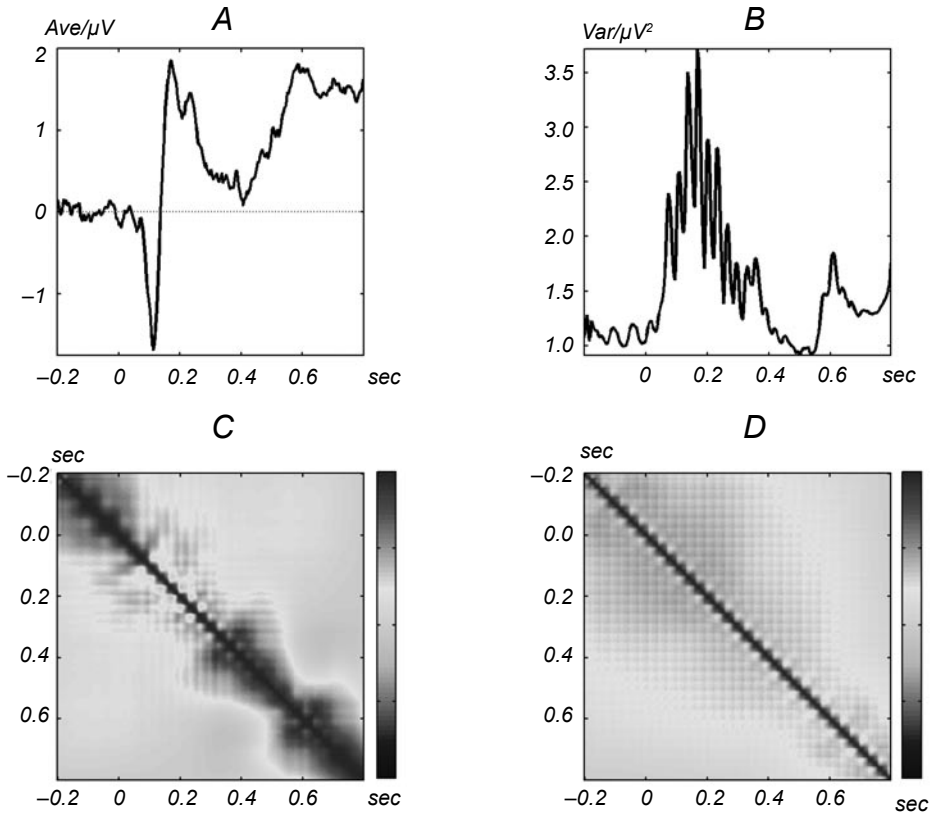

Fig. 1. ERP response to presentation of the critical word of the sentence-processing experiment. A) Grand average as a function of time from the functional mixed-effect regression, B) variance of the grand average, C) correlation matrix showing the within-subject covariance surface (scale indicates the correlation values), and D) correlation matrix of the residual error surface (scale indicates the correlation values).

CWs from approximately 0.3 to 0.5 sec after CW onset, consistent with the N400 effect expected for this contrast. The time points, which exceed the FDR, are all within the expected time range. The effect of trial block appears as a short-duration negative difference near the end of the response interval (Fig. 2B), and the effect associated with the word length appears as a greater positive potential early in the time series (Fig. 2C). Finally, in Fig. 2D, there appears to be no strong evidence of an effect of the word frequency on the response, although there is a weak trend for a negative-potential response at approximately 0.2 sec.

Additional analyses were conducted, including regressors that encoded the interaction of the control/violation contrast with the trial block, word length, and frequency, but no differences exceeding the FDR were obtained for the additional interactions. Also, a model employing crossed random effects for subjects and stimulus items was constructed, similar to the approach outlined by Baayen et al. [5], but no further model improvements were obtained.

DISCUSSION

Functional mixed-effect modeling based on the discrete wavelet transform was used to model the data from a sentence-reading experiment. Posterior samples were used to provide a Bayesian FDR for functional fixed-effect estimates of the ERP contrasts. This analysis illustrates how functional mixed-effect analysis can be used to perform a Bayesian ERP regression. This result is practically relevant for electrophysiology researchers because nearly any combination of linear fixed-effect functions, including factorial contrasts, analysis of covariance, as well as hierarchical or crossed random-effect functions, can be employed to analyze time-series data. In addition, the MCMC approach can be used to obtain estimates

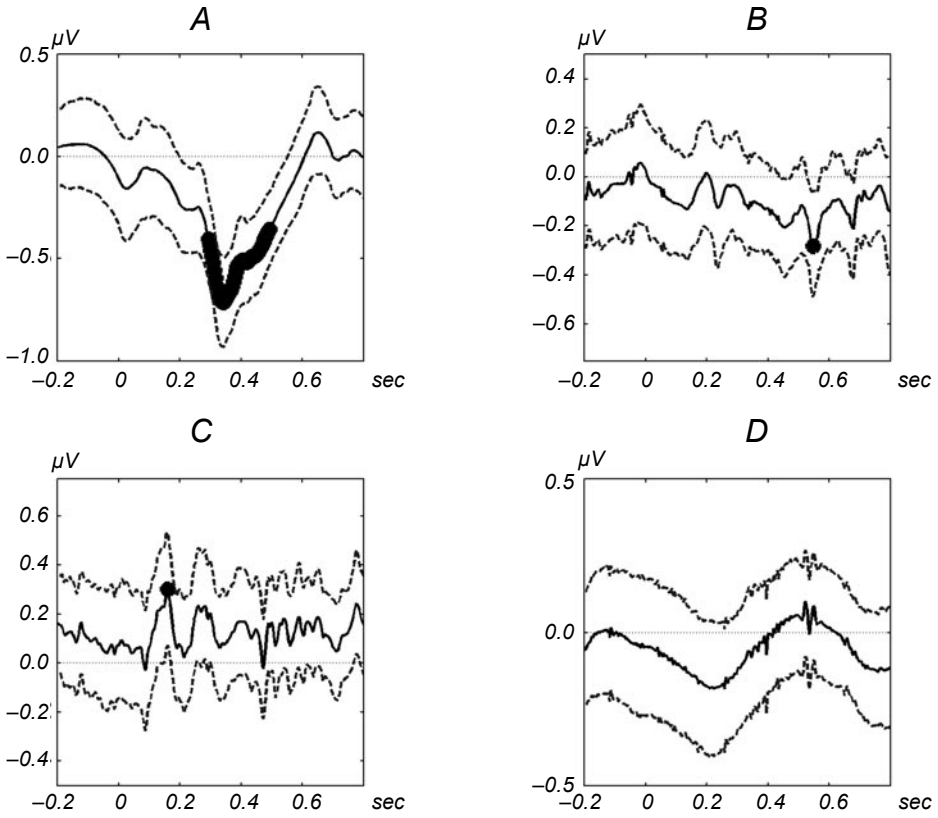

Fig. 2. Functional fixed effects calculated from the regression. Coefficient values as the function of time are plotted as a solid line, zero is indicated with a thin dotted line, upper and lower 95% quantiles are shown as dashed lines, and time points exceeding the false discovery rate are plotted on the mean functions as filled circles. A) Contrast between violation and control, B) trial block, C) word length, and D) word-form frequency.

of the variance and covariance parameters to further elaborate the regression analysis.

Concerning the application results, the contrast between violation and control CWs was obtained within the expected time range, supporting the use of the WFMM approach to detect ordinary experimental effects. The effects of other regressors are consistent with the expectations as well, as the effect of the word length would be expected to affect early stimulus-related activity, while the effect of the trial block would be expected to affect later components of the functional response. The effect of the word frequency was not observed in this data set, but the experiment was not designed to examine the effect of the word frequency *per se*, so the results are not necessarily inconsistent with earlier reports on the word frequency revealed by linear regression by Hauk et al. [28, 29]. For instance, the range of the word frequencies used here is not representative of the range used in the earlier studies, and also the words were presented in the sentence context here.

With respect to EEG analysis in general, there are several potentially limiting assumptions of the WFMM approach, which might be investigated in future research. First, the wavelet transform is assumed to denoise the data because it distributes Gaussian noise over wavelet coefficients. However, unmodeled EEG activity does not consist primarily of Gaussian noise. The dominant feature of the EEG power spectrum is the approximate $1/f$ distribution of the power, often with peaks at certain frequency bands, such as the alpha (8-12 Hz) range. This activity, if it is modeled as noise, would be difficult to separate from the evoked activity with the wavelet approach outlined here because it is not Gaussian; instead, it would be concentrated on a relatively small number of the coefficients. In fact, it has been argued that the DWT is especially effective at modeling these types of the spectra [48, 49]. Note that this limitation is shared by other previous approaches to EEG denoising, which have applied wavelet denoising. However, it is natural to use the wavelet coefficients themselves to investigate the $1/f$ activity, in order to

identify and correct modeling errors. In future work, the distribution of the DWT coefficients themselves could be modeled directly using the same Bayesian approach outlined here, similarly to the non-Bayesian wavelet analysis presented by Davidson and Indefrey [45]. Second, the covariance matrices associated with the wavelet coefficients were assumed to be diagonal, in order to limit the computational complexity of the estimation. Future work might investigate whether a structured covariance matrix would improve the estimation and inference. Finally, it would be useful to explore the effect of the choice of the wavelet basis on the results. Several different basis types have been used in the EEG-related literature, and, as more experience is gained with their statistical properties, it would be useful to assess the effect of a particular selection of the wavelet basis. Also, it is undoubtedly important to establish a rationale for the choice of the wavelet basis based on a forward model for the EEG.

Acknowledgments. This work was supported by grants from the Dutch science foundation Nederlandse Organisatie voor Wetenschappelijk Onderzoek (NWO) and the German science foundation Max Planck Gesellschaft (MPG). Jeff Morris graciously provided the software described in the paper by Morris and Caroll [6], as well as much helpful advice. Any errors in the application of this software to the data reported here are the responsibility of the present author.

REFERENCES

1. G. D. Dawson, A summation technique for detecting small signals in a large irregular background," *J. Physiol*., **115**, 2 (1951).
2. T. C. Handy, *Event-Related Potentials: A Methods Handbook*, MIT Press, Cambridge (2004).
3. L. Sornmo and P. Laguna, *Bioelectric Signal Processing in Cardiac and Neurological Applications*, Elsevier, Academic Press, Amsterdam (2005).
4. J. C. Pinheiro and D. M. Bates, *Mixed-Effects Models in S and S-Plus*, Springer, Berlin (2000).
5. H. Baayen, D. J. Davidson, and D. Bates, "Mixed-effects modeling with crossed random effects for subjects and items," *J. Memory Language*, **59**, 390-412 (2008).
6. J. S. Morris and R. J. Carroll, "Wavelet-based functional mixed models," *J. Roy. Stat. Soc. Ser. B*, **68**, 179-199 (2006).
7. S. G. Mallat, "A theory for multiresolution signal decomposition: The wavelet representation," *IEEE Trans. Pattern Anal. Machine Intell*., **11**, 674-693 (1989).
8. D. B. Percival and A. T. Walden, *Wavelet Methods for Time Series Analysis*, Cambridge Univ. Press, Cambridge (2000).
9. B. Vidakovic, *Statistical Modeling by Wavelets*, Wiley, New York (1999).
10. A. Bruns, "Fourier-, Hilbert- and wavelet-based signal analysis: Are they really different approaches?" *J. Neurosci. Methods*, **137**, 321-332 (2004).
11. M. K. van Vugt, P. B. Sederberg, and M. J. Kahana, "Comparison of spectral analysis methods for characterizing brain oscillations," *J. Neurosci. Methods*, **162**, 49-63 (2007).
12. V. J. Samar, K. P. Swartz, M. R. Raghuveer, "Multiresolution analysis of event-related potentials by wavelet decomposition," *Brain Cognition*, **27**, 398-438 (1995).
13. O. Bertrand, J. Bohorquez, and J. Pernier, "Time-frequency digital filtering based on an invertible wavelet transform: An application to evoked potentials," *IEEE Trans. Biomed. Eng.*, **41**, 77-88 (1994).
14. E. A. Bartnik, K. J. Blinowska, P. J. Durka, "Single evoked potential reconstruction by means of wavelet transform," *Biol. Cybern.*, **67**, 175-181 (1992).
15. N. V. Thakor, G. Xin-Rong, S. Yi-Chun, and D. F. Hanley, "Multiresolution wavelet analysis of evoked potentials," *IEEE Trans. Biomed. Eng.*, **40**, 1085-1094 (1993).
16. T. Demiralp, J. Yordanova, V. Kolev, et al., "Time-frequency analysis of single-sweep event-related potentials by means of fast wavelet transform," *Brain Language*, **66**, 129-145 (1999).
17. S. J. Kiebel and K. J. Friston, "Statistical parametric mapping for event-related potentials (II): A hierarchical temporal model," *Neuroimage*, **22**, 503-520 (2004).
18. J. Raz, B. I. Turetsky, and L. W. Dickerson, "Inference for a random wavelet packet model of single-channel event-related potentials," *J. Am. Statist. Assoc.*, **96**, 409-420 (2001).
19. X. F. Wang, Q. Yang, Z. Fan, et al., "Assessing time-dependent association between scalp EEG and muscle activation: A functional random-effects model approach," *J. Neurosci. Methods*, **177**, 232-240 (2009).
20. D. L. Donoho and I. M. Johnstone, "Minimax estimation via wavelet shrinkage," *Annu. Statistics*, **26**, 879-921 (1998).
21. R. Quian Quiroga and H. Garcia, "Single-trial event-related potentials with wavelet denoising," *Clin. Neurophysiol*., **114**, 376-390 (2003).
22. Z. Wang, A. Maier, D. A. Leopold, et al., "Single-trial evoked potential estimation using wavelets," *Comput. Biol. Med*., **37**, 463-473 (2007).
23. A. Effern, K. Lehnertz, T. Grunwald, et al., "Time adaptive denoising of single trial event-related potentials in the wavelet domain," *Psychophysiology*, **37**, 859-865 (2000).
24. A. Effern, K. Lehnertz, G. Fernandez, et al., "Single trial analysis of event-related potentials: Non-linear denoising with wavelets," *Clin. Neurophysiol*., **111**, 2255-2263 (2000).
25. A. Effern, K. Lehnertz, T. Schreiber, et al., "Nonlinear denoising of transient signal with application to event related potentials," *Physica D*, **140**, 257-266 (2000c).
26. B. M. Sayers, H. A. Beagley, and W. R. Henshall, "The mechanism of auditory evoked EEG responses," *Nature*, **247**, 481-483 (1974).
27. E. Basar, *EEG-Brain Dynamics: Relation between EEG and Brain Evoked Potentials*, Elsevier, New York (1980).

28. O. Hauk and F. Pulvermüller, "Effects of word length and frequency on the human event-related potential," *Clin. Neurophysiol.*, **115**, 1090-1103 (2004).
29. O. Hauk, M. H. Davis, M. Ford, et al., "The time course of visual word recognition as revealed by linear regression analysis of ERP data," *Neuroimage*, **30**, 1383-1400 (2006).
30. S. G. Costafreda, G. J. Barker, and M. J. Brammer, "Bayesian wavelet-based analysis of functional magnetic resonance time series," *Magn. Res. Imaging*, Nov. 5 (2008).
31. M. J. Fadili and E. T. Bullmore, "A comparative evaluation of wavelet-based methods for hypothesis testing of brain activation maps," *Neuroimage*, **23**, 1112-1128 (2004).
32. L. Sendur, J. Suckling, B. Whitcher, and E. Bullmore, "Resampling methods for improved wavelet-based multiple hypothesis testing of parametric maps in functional MRI," *Neuroimage*, **37**, 1186-1194 (2007).
33. G. A. Miller, W. Lutzenberger, and R. Ulrich, "A jackknife-based method for measuring LRP onset latency differences," *Psychophysiology*, **35**, 99-115 (1998).
34. D. Guthrie and J. S. Buchwald, "Significance testing of difference potentials," *Psychophysiology*, **28**, 240-244 (1991).
35. R. C. Blair and W. Karniski, "An alternative method for significance testing of waveform difference potentials," *Psychophysiology*, **30**, 518-524 (1993).
36. A. Achim, "Signal detection in averaged evoked potentials: Monte Carlo comparison of the sensitivity of different methods," *Electroencephalogr. Clin. Neurophysiol.*, **96**, 574-584 (1995).
37. E. Maris and R. Oostenveld, "Nonparametric statistical testing of EEG- and MEG-data," *J. Neurosci. Methods*, **164**, 177-190 (2007).
38. N. Laird and J. H. Ware, "Random-effects models for longitudinal data," *Biometrics*, **38**, 963-974 (1982).
39. W. S. Guo, "Functional mixed effect models," *Biometrics*, **58**, 121-128 (2002).
40. A. Antoniadis and T. Sapatinas, "Estimation and inference in functional mixed-effects models," *Comput. Stat. Data Anal.*, **51**, 4793-4813 (2007).
41. F. Abramovich, A. Antoniadis, T. Sapatinas, and B. Vidakovic, "Optimal testing in a fixed effects functional analysis of variance model," *Int. J. Wavelets, Multiresolution Inform. Proc.*, **2**, 323-349 (2004).
42. C. Bugli and P. Lambert, "Functional ANOVA with random functional effects: an application to event-related potentials modeling for electroencephalograms analysis," *Stat. Med.*, **25**, 3718-3739 (2006).
43. A. P. Dawid, "Some matrix-variate distribution theory: Notational considerations and a Bayesian application," *Biometrika*, **68**, 265-274 (1981).
44. J. S. Morris, P. J. Brown, R. C. Herrick, et al., "Bayesian analysis of mass spectrometry proteomic data using wavelet based functional mixed models," *Biometrics*, **64**, 479-489 (2008).
45. D. J. Davidson and P. Indefrey, "An inverse relation between event-related and time-frequency violation responses in sentence processing," *Brain Res.*, **1158**, 81-92 (2007).
46. M. Kutas and S. A. Hillyard, "Reading senseless sentences: Brain potentials reflect semantic incongruity," *Science*, **207**, 203-205 (1980).
47. R. H. Baayen, R. Piepenbrock, and L. Gulikers, *The CELEX Lexical* Functional mixed effects 27 *Database (Release 2)* [CD-ROM], Philadelphia, PA: Linguistic Data Consortium, University of Pennsylvania [Distributor]. (1995).
48. G. W. Wornell, *Signal Processing with Fractals: A Wavelet-Based Approach*, Upper Saddle River, NJ, Prentice-Hall. (1996).
49. E. Bullmore, C. Long, J. Suckling, J., et al., "Colored noise and computational inference in neurophysiological (fMRI) time series analysis: Resampling methods in time and wavelet domains," *Human Brain Mapping*, **12**, 61-78 (2001).